3rd AIAA Flow Control Conference
5 - 8 June 2006, San Francisco, California

AIAA 2006-3345

Discrete Adjoint Formulation for the Ideal MHD Equations

Andre C. Marta*, Juan J. Alonso†
Stanford University, Stanford, CA 94305

For over twenty years there has been computational work to analyze and control hypersonic flows using electromagnetic effects but no true effort has been pursued to automate the flow control process. The lack of a design framework that provides automated multidisciplinary optimization (MDO) capabilities for this class of problems is the principal motivation for this work. This paper extends the foundation of a MDO component previously developed by the authors to the ideal MHD equations that govern the three-dimensional flow of an inviscid compressible perfectly conducting fluid with an externally imposed magnetic field. The gas is assumed perfect and chemically frozen, as the focus is on the discrete adjoint derivations rather than on the flow solver. Control theory has already been proved successful dealing with both aerodynamic shape and magnetohydrodynamics (MHD) optimization using an inviscid low magnetic Reynolds number model by the authors. The discrete adjoint is the best suitable option to deal with the complex equations that govern MHD, and with the nature of the cost functions that may be used for relevant design problems. At this point, the derivation of the adjoint system of equations is done by hand differentiation of the flow solver. The sensitivities computed using the discrete adjoint formulation are matched against values obtained using finite-differences and a sample design problem is presented. On going work includes the incorporation of non-ideal effects in the governing equations, parallelization of both the flow and the adjoint solvers and the use of automatic differentiation tools to effortlessly compute the adjoint system of equations from the coded flow solver. Once all this is accomplished, the investigation of meaningful design problems and the definition of significant cost functions will finally be tackled.

I. Introduction

Since the moment the Wright brothers debuted the first powered, heavier-than-air machine that achieved controlled and sustained flight, back in 1903, a quest for faster and faster aircrafts took place. More than one hundred years went by and the transonic and supersonic frontiers have been crossed, however, the hypersonic regime still poses challenging problems. The interest in hypersonic flight has led to an extensive number of conceptual studies[1,2] but it was not until 2004 that the first successful hypersonic flights of a vehicle with an air-breathing engine took place.[3] It is clear that many technical and scientific obstacles still remain in order to reach a stage in which hypersonic flight enters our daily life.

When the air flows at hypersonic speeds around blunt bodies, very strong detached shock waves emerge in the regions of intense flow deceleration. There, much of the mean flow kinetic energy is converted into internal energy, namely translational and vibrational energy, which causes the temperature of the air to

*Doctoral Candidate, AIAA Member
†Associate Professor, AIAA Member

increase dramatically. In turn, this temperature increase leads to the dissociation and ionization of the air. The plasma produced under such conditions allows for the flow control using magnetic fields.

The analysis of plasma flows under the presence of magnetic fields is designated as magnetohydrodynamics (MHD). In order to cope with the extreme complexity of the full MHD analysis, several simplified models have been developed. The problem might first be approach ignoring the viscous effects and the heat transfer, as well as no electrostatic force, no displacement current and no resistivity, the MHD equations reduce to the ideal MHD formulation.[4] Also, low magnetic Reynolds number approximations make the solution of the magnetic field unnecessary,[5] since the magnetic field is assumed to be decoupled from the velocity field. If chemical reactions are taken into account, the chemical model of reacting gas has to be included in the governing equations, which dramatically increases the computational cost .[6]

There has been some work done trying to analyze and control the flow in scramjet inlets using MHD [7,8] but no true effort has come out to automate the control process. In order to tackle this deficiency, the authors have already built a design framework[9] which provides automated optimization capabilities using the inviscid low magnetic Reynolds number MHD model. The control theory approach, also called the adjoint method, was used to efficiently obtain the gradient information required by the optimizer in the design framework. A discrete adjoint formulation was used and it successfully demonstrated the feasibility of such an approach, in which up to thousands of design variables were used. The discrete adjoint formulation might be harder to derive, if done by hand, but it produces gradients that are consistent with the flow solver. In addition, it can be applicable to arbitrarily complex governing equations and cost/constraint functions.

The goal of the present work is to extend the discrete adjoint theory to the control of an inviscid hypersonic flow in the presence of strong magnetic fields using the ideal MHD equations, in which the magnetic induction equations play an important role.

In the following sections we describe the various components of the design method that we have developed. We start with the description of the physical model, in particular the governing equations of the hypersonic flow under the influence of magnetic fields, and the discrete adjoint formulation. We then provide details of the numerical models used, both for the flow solution and the adjoint solution. Next, some results are presented, both the verification of the gradients obtained with the discrete adjoint approach and a sample problem using the design framework. Lastly, some remarks are made concerning steps that will by taken in the future to achieve a more robust, powerful and accurate framework.

II. MHD Governing Equations

The equations governing the three-dimensional flow of an inviscid, compressible, perfectly conducting fluid in a magnetic field are obtained by coupling the Navier-Stokes equations to the Maxwell equations. The viscous terms of the Navier-Stokes equations and the dispersive terms of the induction equations are neglected in this model. The resulting ideal MHD equations can be expressed in various mathematical forms but the conservation-law form is often preferred for numerical models. This set of equations explicitly represent conservation of mass, momentum, total energy, and induction of the magnetic field and, under certain assumptions,[10] it is given by

$$\frac{\partial \mathbf{U}}{\partial t} + \nabla \cdot \mathbf{F} = 0. \tag{1}$$

Here $\mathbf{U}$ represents the vector of conservative variables and $\mathbf{F}$ is the inviscid flux. In non-dimensional form, these are

$$\mathbf{U} = \begin{pmatrix} \rho \\ \rho\mathbf{u} \\ \rho Z \\ \mathbf{B} \end{pmatrix} \quad \text{and} \quad \mathbf{F} = \begin{pmatrix} \rho\mathbf{u} \\ \rho\mathbf{u}\mathbf{u} + P\mathbf{I} - R_b(\mathbf{B}\mathbf{B}/\mu_m) \\ (\rho Z + P)\mathbf{u} - R_b(\mathbf{u}\cdot\mathbf{B}/\mu_m)\mathbf{B} \\ \mathbf{u}\mathbf{B} - \mathbf{B}\mathbf{u} \end{pmatrix}.$$

The conservative variables are the density ρ, the momentum density $\rho\mathbf{u}$, the total energy density ρZ, and the magnetic field $\mathbf{B}$, with the energy equation derived by introducing the variable

$$Z = E + R_b \frac{\mathbf{B}\cdot\mathbf{B}}{2\mu_m\rho}, \tag{2}$$

where the total energy E is expressed in terms of internal and kinetic energy as

$$E = e + \frac{1}{2}\mathbf{u}\cdot\mathbf{u}. \tag{3}$$

Similarly, the modified pressure P is given by the sum of the static pressure and the magnetic pressure as

$$P = p + R_b \frac{B^2}{2\mu_m}, \tag{4}$$

where μ_m is the magnetic permeability.

One non-dimensional parameter is formed in this formulation, namely the the magnetic force number

$$R_b = \frac{B_{ref}^2}{\rho_{ref} U_{ref}^2 \mu_{m_{ref}}}. \tag{5}$$

This ideal MHD model allows for environments characterized by a high magnetic force number, where the magnetic field induced by the current is of comparable magnitude to the one imposed on the flow, since the three induction equations are solved in the governing equations, as opposed to the low magnetic Reynolds number model.[5] In the present work, the flow is assumed to be frozen so chemical reactions are neglected.

According to the Gauss' law for magnetism, the magnetic field have to satisfy the solenoidal condition

$$\nabla\cdot\mathbf{B} = 0. \tag{6}$$

Recalling that the transient evolution of the magnetic field is governed by Faraday's law,

$$\frac{\partial\mathbf{B}}{\partial t} = -c\nabla\times\mathbf{E}, \tag{7}$$

since $\nabla\cdot(\nabla\times\mathbf{E}) = 0$, equation (7) implies that $\nabla\cdot\mathbf{B}$ is independent of time.[11] Therefore, the exact solution of the MHD equations (1) keeps the condition (6) indefinitely if it is satisfied initially. However, in numerical MHD simulations, not only round-off errors but also the use of artificial dissipation schemes lead to a finite divergence of the magnetic field, thus violating that condition and not preserving the differential property of $\nabla\cdot\mathbf{B}$. Among others, Brackbill[12] has shown that even very small errors in satisfying equation (6) cause large errors in the solution of the MHD equations (1).

There are different approaches to enforce the solenoidal condition (6) but in the present work, the inclusion of additional source terms has been used. The derivation of the ideal MHD equations (1) is done assuming

that terms proportional to $\nabla \cdot \mathbf{B}$ are zero analytically. Had this not been done, there would be extra source terms on the right-hand, as in the derivations of both Panofsky[13] and Vinokur[14]

$$\mathbf{S} = -\nabla \cdot \mathbf{B} \begin{pmatrix} 0 \\ R_b \mathbf{B}/\mu_m \\ R_b \left(\mathbf{U} \cdot \mathbf{B}\right)/\mu_m \\ \mathbf{U} \end{pmatrix}. \tag{8}$$

Both Powell[10] and Tóth[15] have found that including these corrective terms stabilizes and improves the solution. It should be noted that the terms are non-conservative; thus conservation of momentum, energy, and magnetic flux are not strictly enforced any longer.

Besides the issue of satisfying the solenoidal condition (6), there is also the problem of having large imposed magnetic fields. Under these circumstances, the ratio of induced to imposed components of the magnetic field becomes extremely small and the magnetic terms can dominate the system. Small errors in the magnetic field solution can cause severe difficulties in the energy equation, because the magnetic energy becomes much greater than the kinetic energy.

Following the work of Tanaka,[16] this problem can be mitigated by decomposing the magnetic field $\mathbf{B}$ into two components, the background imposed field $\mathbf{B}_0$ and the induced field $\mathbf{B}_i$ as

$$\mathbf{B} = \mathbf{B}_0 + \mathbf{B}_i. \tag{9}$$

The decomposition (9) allows for the derivation of MHD governing equations that avoid the direct inclusion of the imposed components of the magnetic field as dependent variables, when the imposed magnetic field satisfies the conditions

$$\begin{aligned} \frac{\partial \mathbf{B}_0}{\partial t} &= 0 \quad , \\ \nabla \cdot \mathbf{B}_0 &= 0 \quad \text{and} \\ \nabla \times \mathbf{B}_0 &= 0 \end{aligned} \tag{10}$$

. These conditions mean that the imposed magnetic field $\mathbf{B}_0$ is steady, satisfies the Gauss' law for magnetism, and is produced outside of the flow domain (no current sources in the domain), respectively.

Introducing a new set of dependent variables $\mathbf{U}_i = (\rho, \rho\mathbf{u}, \rho Z_i, \mathbf{B}_i) = (\rho, \rho\mathbf{u}, \rho Z - R_b(\mathbf{B}_i \cdot \mathbf{B}_0)/(\mu_m) - R_b B_0^2/(2\mu_m), \mathbf{B} - \mathbf{B}_0)$, the governing equations (1) and (8), together with the conditions (10), result in the conservative system of ideal MHD equations[15] used in this work:

$$\frac{\partial \mathbf{U}_i}{\partial t} + (\nabla \cdot \mathbf{F}_i) + (\nabla \cdot \mathbf{G}) = \mathbf{S}_i. \tag{11}$$

where

$$\mathbf{U}_i = \begin{pmatrix} \rho \\ \rho\mathbf{u} \\ \rho Z_i \\ \mathbf{B}_i \end{pmatrix}, \qquad \mathbf{F}_i = \begin{pmatrix} \rho\mathbf{u} \\ \rho\mathbf{u}\mathbf{u} + P_i\mathbf{I} - R_b(\mathbf{B}_i\mathbf{B}_i)/\mu_m \\ (\rho Z_i + P_i)\mathbf{u} - R_b(\mathbf{u} \cdot \mathbf{B}_i)\mathbf{B}_i/\mu_m \\ \mathbf{u}\mathbf{B}_i - \mathbf{B}_i\mathbf{u} \end{pmatrix},$$

$$\mathbf{G} = \begin{pmatrix} 0 \\ (\mathbf{B}_0 \cdot \mathbf{B}_i)\mathbf{I} - R_b(\mathbf{B}_0\mathbf{B}_i + \mathbf{B}_i\mathbf{B}_0)/\mu_m \\ R_b(\mathbf{B}_0 \cdot \mathbf{B}_i)\mathbf{u}/\mu_m - R_b(\mathbf{u} \cdot \mathbf{B}_i)\mathbf{B}_0/\mu_m \\ \mathbf{u}\mathbf{B}_0 - \mathbf{B}_0\mathbf{u} \end{pmatrix} \text{ and } \quad \mathbf{S}_i = -\nabla \cdot \mathbf{B}_i \begin{pmatrix} 0 \\ R_b\mathbf{B}/\mu_m \\ R_b\left(\mathbf{u} \cdot \mathbf{B}_i\right)/\mu_m \\ \mathbf{u} \end{pmatrix}.$$

The energy ρZ_i, density ρ, momentum $\rho\mathbf{u}$ and magnetic field $\mathbf{B}_i$ are related to pressure p by

$$p = (\gamma - 1)\left(\rho Z_i - \frac{1}{2}\rho u^2 - R_b \frac{B_i^2}{2\mu_m}\right), \tag{12}$$

where the ideal gas assumption was made and γ is the ratio of the constant pressure and constant volume heat coefficients.

It is relevant to mention that the splitting (9) makes no assumption about the relative size of $\mathbf{B}_0$ and $\mathbf{B}_i$; the only requirement is that the imposed magnetic field satisfies (10).

III. Discrete Adjoint Formulation

The control theory approach has been used extensively in the last years for both aerodynamic shape optimization and aero-structural design[17] and has recently also been proved successful in MHD design.[9] This approach is well known for its capability to effectively handle design problems involving a large number of design variables and a few number of objective functions. The sensitivities are obtained by solving a system of equations of size equivalent to the governing equations of the flow. When compared to traditional finite-difference methods, the adjoint approach enables large computational savings, at the expense of a more complex implementation.[18] This work employs a discrete adjoint formulation, meaning that the adjoint system of equations is obtained by differentiating the discretized form of the governing equations.

Let $\mathbf{U}$ be the set of all flow variables at discrete grid points arising from an approximate solution of the governing equations, α the set of design variables which influence the flow, and J the scalar function which approximates the desired cost function. Then, in the context of control theory, the design problem can be posed as

$$\begin{aligned} &\textit{Minimize} && J(\mathbf{U},\alpha) \\ &\textit{w.r.t.} && \alpha, \\ &\textit{subject to} && R(\mathbf{U},\alpha) = 0 \\ & && C_i(\mathbf{U},\alpha) = 0 \qquad i = 1,...,m \end{aligned} \tag{13}$$

where $R(\mathbf{U},\alpha) = 0$ represents the discrete flow equations and boundary conditions that must be satisfied and $C_i(\mathbf{U},\alpha) = 0$ are m additional constraints.

When using a gradient-based optimizer to solve the problem (13), the sensitivity of both the cost function J and the constraints C_i with respect to the design variables are required. By constructing the adjoint system of equations (14) and solving for the adjoint variables λ

$$\left[\frac{\partial R}{\partial U}\right]^T \lambda = \left[\frac{\partial J}{\partial U}\right]^T, \tag{14}$$

the sensitivity of the cost function is simply given by

$$\frac{dJ}{d\alpha} = \frac{\partial J}{\partial \alpha} - \lambda^T \frac{\partial R}{\partial \alpha}. \tag{15}$$

An additional adjoint system has to be solved for each additional constraint function C, which implies computing a new right-hand side for the system (14).

The sensitivity obtained from (15) can then be used to find the search direction of the gradient based optimization algorithm as indicated in figure 1.

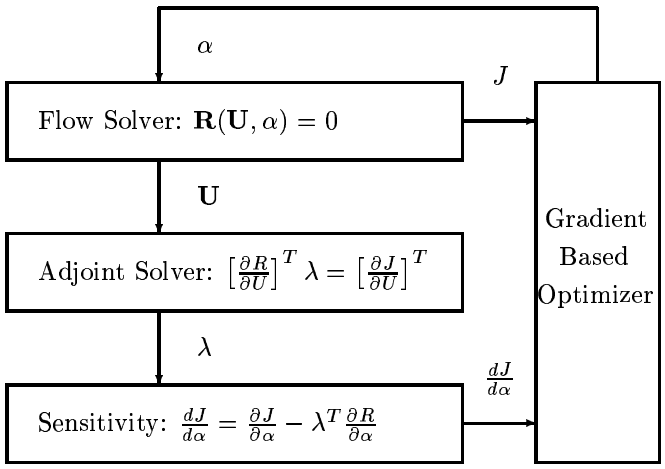

Figure 1. Schematic of the adjoint-based optimization algorithm.

The advantage of the adjoint approach can be seen from equation (15), which is independent of δU, meaning that the gradient of J with respect to an arbitrary large vector of design variables α can be determined without the need for additional flow-field evaluations.

Additional details about the discrete adjoint approach and its implementation can be found in the authors previous work.[9]

IV. Numerical Model

A. MHD Solver

The hyperbolic system of partial-differential equations governing the ideal MHD flow (11) is solved using a cell-centered finite-volume discretization scheme on a structured mesh of hexahedral cells. This produces a system of ordinary differential equations (ODE), where in each cell holds

$$\frac{d}{dt}(V_{ijk}\mathbf{U}_{ijk})+\mathbf{R}_{ijk}=0, \tag{16}$$

where V_{ijk} is the cell volume, and $\mathbf{R}_{ijk}$ is the net flux out of the computational cell (i,j,k) computed as

$$\mathbf{R}_{ijk}=\sum_{faces}\mathbf{F}\cdot d\mathbf{S}+\sum_{faces}\mathbf{G}\cdot d\mathbf{S}+\sum_{faces}\mathbf{B}_i\cdot d\mathbf{S}\begin{pmatrix}0\\ R_b\mathbf{B}/\mu_m\\ R_b\left(\mathbf{U}\cdot\mathbf{B}_i\right)/\mu_m\\ \mathbf{U}\end{pmatrix}. \tag{17}$$

The resulting set of coupled ODEs (16) is integrated in time using an explicit multi-stage modified Runge-Kutta scheme to steady state. The time step is restricted by the Courant-Friedrichs-Levy (CFL) condition,

$$\Delta t <= Cmin\left(\frac{\Delta h}{\lambda_n^{max}}\right), \tag{18}$$

where C is the Courant number, h is the cell spacing and λ_n^{max} is the maximum propagation speed of information in the direction normal to the computational cell face, that corresponds to the maximum eigenvalue of the hyperbolic system of ideal MHD equations (11).

According to Powell,[19] the system (11) has eight distinct eigenvalues, namely the entropy, magnetic-flux, Alfvèn, fast and slow magneto-acoustic waves, corresponding the maximum eigenvalue to the fast magneto-acoustic wave

$$\lambda_{max} = |U_n| + c_f, \tag{19}$$

where U_n is the normal fluid velocity and c_f is the speed of the fast-mode MHD wave, relative to the fluid, which is given by

$$c_f = \sqrt{\frac{1}{2}\left[c^2 + \frac{B^2}{\rho\mu_m} + \sqrt{\left(c^2 + \frac{B^2}{\rho\mu_m}\right)^2 - 4\frac{c^2 B_n^2}{\rho\mu_m}}\right]}, \tag{20}$$

with the speed of sound defined as $c = \sqrt{\frac{\gamma p}{\rho}}$.

The maximum eigenvalue (19) is also used in the numerical artificial dissipation scheme.

B. Discrete Adjoint Solver

The discrete adjoint system of equations (14) is constructed by differentiating all the numerical fluxes that comprise the residual R_{ijk} of the discretized governing equations (17). In the present paper, that is accomplished by manual differentiation of the flux routines of the MHD flow solver.

Since a structured mesh is used, the adjoint system of equations is multi-diagonal block matrix whose number of non-zero diagonals matches the dimension of the stencil used in the flow solver. For the present discretization, a stencil of seven cells is used. The details of how the non-zero block matrix entries of $\frac{\partial R}{\partial U}$ and $\frac{\partial J}{\partial U}$ are computed follows the procedure outlined in the previously published work.[9]

Special care is taken at the boundaries, where the cells have stencils that extend outside the internal computational domain. There, the chain rule is used to take into account the dependence of the halo cells on the interior cells, according to the type of boundary condition used in the flow solver.

As an illustration, consider a cell at the boundary $i_{min} = 2$. In this case, the value of the conservative vector $\mathbf{U}$ at the halo cell $i = 1$ is a function of the interior cells $\mathbf{U}_{i=1} = f(\mathbf{U}_{i=2}, \mathbf{U}_{i=3})$. Therefore, there is an additional contribution to the block matrices corresponding to the Jacobian of the residual at cell $i_{min} = 2$, given as

$$\begin{aligned}
\mathcal{B}_{i=2}(m,n) = \frac{\partial R_{i=2}(m)}{\partial U_{i=1}(n)} &= 0 \\
\mathcal{A}_{i=2}(m,n) = \frac{\partial R_{i=2}(m)}{\partial U_{i=2}(n)} &= \frac{\partial R_{i=2}(m)}{\partial U_{i=1}(l)}\frac{\partial U_{i=1}(l)}{\partial U_{i=2}(n)} \\
\mathcal{C}_{i=2}(m,n) = \frac{\partial R_{i=2}(m)}{\partial U_{i=3}(n)} &= \frac{\partial R_{i=2}(m)}{\partial U_{i=1}(l)}\frac{\partial U_{i=1}(l)}{\partial U_{i=3}(n)},
\end{aligned} \tag{21}$$

where the auxiliary Jacobians $\frac{\partial U_{i=1}}{\partial U_{i=2}}$ and $\frac{\partial U_{i=1}}{\partial U_{i=3}}$ are obtained from the flow solver boundary condition routines.

In order to solve the large discrete adjoint matrix problem (14), the Portable, Extensible Toolkit for Scientific Computation (PETSc) [20] is used. Due to the structure of the matrix to be solved, a sparse storage is selected. The system is solved using the GMRES algorithm in conjunction with an incomplete LU factorization preconditioner. Once the adjoint solution is found, the gradient of the function of interest is easily obtained from equation (15).

C. Gradient-Based Optimizer

The optimization problem is solved by feeding the cost and constraint function values, obtained by the MHD solver, and their gradients, obtained by the adjoint solver, into a gradient-based optimizer. The optimizer used in this work is SNOPT ,[21] which is a software package for solving large-scale optimization problems.

V. Problem Set-Up and Control Variables

The configuration used in this paper consists of a blunt cylinder immersed in an hypersonic incoming flow, at an arbitrary angle of attack and side slip angle. These two angles are design (control) variables in the optimization problem.

A. Imposed Magnetic Field

A collection of hypothetical electric circuits is placed inside the body which imposes a magnetic field on the flow. Each elementary circuit is thought to produce a dipole like magnetic field given by

$$\mathbf{B} = \frac{\mu_m m}{4\pi r^3} \left[2\cos\theta \mathbf{e}_r + \sin\theta \mathbf{e}_\theta \right], \tag{22}$$

where r and θ define the dipole orientation and m is the dipole strength. This way, three additional control variables are inserted in the design problem - dipole strength and orientation (two angles) - for each dipole placed inside the body. The location of the dipoles is defined by the user and kept fixed.

B. Body Shape

A collection of bumps is located on the body nose so that shape control can be performed. These bumps are given by Hicks-Henne functions,[22] whose amplitudes are considered control variables. The location of the bumps is defined by the user and kept fixed.

VI. Results

In this section, a verification study of the sensitivities provided by the discrete adjoint formulation is presented. For this purpose, finite-difference sensitivities obtained from the flow solver are used. Additionally, a sample design case using the sensitivity information obtained with the adjoint approach is also shown.

A. Sensitivity Verification

A baseline configuration consisting of the blunt body described in the previous section, with a single dipole located at the body nose center, oriented against a Mach 5 incoming flow at an angle of attack of 20° and side-slip angle of 5° is modeled using a 32x32x64 mesh. The baseline design variable values are included in table 3.

The plots in figure 2 show both the imposed magnetic field due to the embedded dipole, and the induced magnetic field computed by the ideal MHD flow solver, on a vertical plane, where the contour map represents the magnetic field magnitude and the streamlines show the magnetic field vector. The expected strong bow shock is captured in figure 3, in which the Mach number is plotted, together with the static pressure distribution.

Figure 4 shows the drag and lift coefficient sensitivities with respect to 7 design variables - angle of attack, side-slip angle, bump amplitudes (2) and dipole strength (1) and orientation (2). The sensitivities obtained

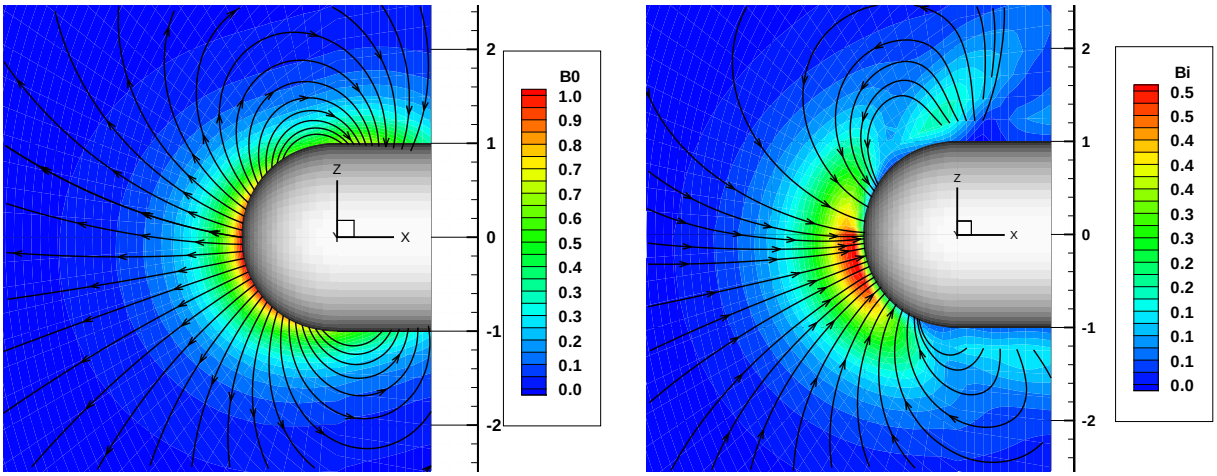

(a) Imposed field

(b) Induced field

Figure 2. Magnetic field distribution for baseline configuration on a vertical plane.

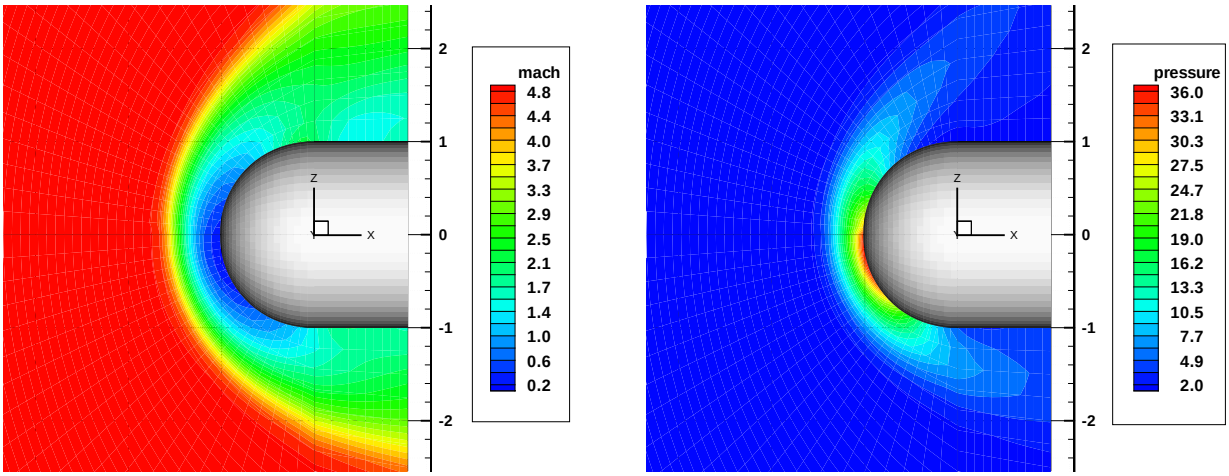

(a) Mach number

(b) Static pressure

Figure 3. Baseline solution on a vertical plane.

using the discrete adjoint approach are matched against values obtained using a finite-difference solution, with a perturbation step of 10^{-5} for the design variables, and the results are summarized in table 1.

In general, there is an excellent agreement between the two approaches. The differences that sometimes occur are thought to be due to either the inaccuracy of the finite-difference solution itself or to some approximations computing the vector $\frac{dJ}{d\alpha}$ and the matrix $\frac{\partial R}{\partial \alpha}$ in equation (15).

The computational times necessary to obtain these verification results are shown in table 2, where the CPU time required to obtain to solve the adjoint system of equations is used as reference. The flow solution was obtained from a cold start (free-stream conditions in the whole domain), while the finite-difference solver

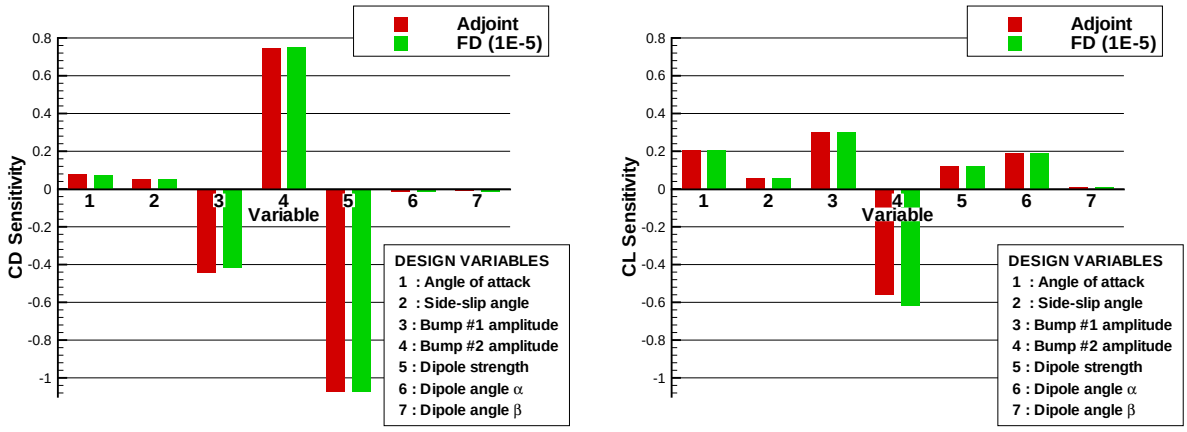

Figure 4. Drag and lift coefficient sensitivities.

	Drag Coefficient			Lift Coefficient		
Design Variable	Adjoint	Finite-Diff.	Δ	Adjoint	Finite-Diff.	Δ
Angle of attack	$7.461E-2$	$7.432E-2$	0.4%	$2.044E-1$	$2.044E-1$	0.0%
Side-slip angle	$4.871E-2$	$4.863E-2$	0.2%	$5.846E-2$	$5.839E-2$	0.1%
Bump #1 amplitude	$-4.432E-1$	$-4.146E-1$	6.9%	$3.021E-1$	$3.005E-1$	0.5%
Bump #2 amplitude	$7.447E-1$	$7.504E-1$	-0.8%	$-5.572E-1$	$-6.164E-1$	-9.6%
Dipole strength	$-1.070E+0$	$-1.071E+0$	-0.1%	$1.186E-1$	$1.186E-1$	0.1%
Dipole angle α	$-1.526E-2$	$-1.527E-2$	0.0%	$1.869E-1$	$1.869E-1$	0.0%
Dipole angle β	$-1.003E-2$	$-1.064E-2$	-5.7%	$7.790E-3$	$7.790E-3$	0.0%

Table 1. Sensitivity verification.

used the previously computed flow solution as initial guess, having to converge only due to the design variable perturbation. The CPU time of the adjoint solution is nearly independent of the number of design variables, but dependent on the number of cost functions, whereas the CPU time of the finite-difference approach is approximately linearly dependent on the number of design variables and independent of the number of cost functions. These timings clearly demonstrate the excellent efficiency of the adjoint-based sensitivity approach when compared to the traditional finite-difference approach, here with a 43:1 ratio. Obviously, the finite-difference approach handicap would have been even larger if more design variables had been used.

Solver	time
Flow	21
Adjoint	1
Finite-differences	43

Table 2. Computational time with 2 cost functions and 7 design variables.

B. Sample Design Problem

To demonstrate the design capabilities achieved by using the sensitivity information obtained by the discrete adjoint approach, a simple design problem of the form (13) is solved using the same body set-up. The design problem intends to control the drag coefficient, either minimize or maximize it, while keeping the lift coefficient within a specified range. The range and baseline values of the design variables and constraints are shown in table 3.

Figure 5 shows the convergence history of the design iterations for both the drag minimization and maximization cases. The optimizer quickly drives the design solution toward the optimum and then further iterates to achieve the desired accuracy. As expected, the minimum drag optimal solution corresponds to a slender body with a weak imposed magnetic field, while the maximum drag optimal solution corresponds to a more blunt body with a strong imposed magnetic field, as sketched in figure 6. The optimal results obtained for both cases are also summarized in table 3. In both design problems, the optimal solutions satisfy all the constraints and significant improvement is achieved over the baseline configuration.

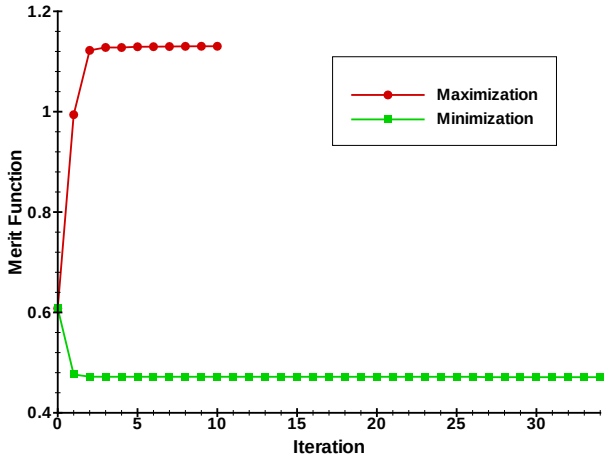

Figure 5. Merit function convergence history.

Design Variable	x_{min}	x_0	x_{max}	CD_{min}	CD_{max}
Angle of attack	−0.3491	0.1745	0.3491	0.0761	0.2349
Side-slip angle	−0.1745	0.0858	0.1745	0.0000	0.0272
Bump #1 amplitude	0.1000	0.2000	0.3000	0.3000	0.1000
Bump #2 amplitude	0.0500	0.1000	0.1500	0.0500	0.1500
Dipole strength	−0.1200	−0.0100	−0.0100	−0.0100	−0.1200
Dipole angle α	−0.6981	0.0853	0.6981	0.6981	0.2412
Dipole angle β	−0.3491	0.1745	0.3491	0.0029	0.0372
Drag Coefficient	–	0.6080	–	0.4710	1.1304
Lift Coefficient	0.0350	0.0385	0.0400	0.0350	0.0350

Table 3. Design variable bounds, initial value and optimal values.

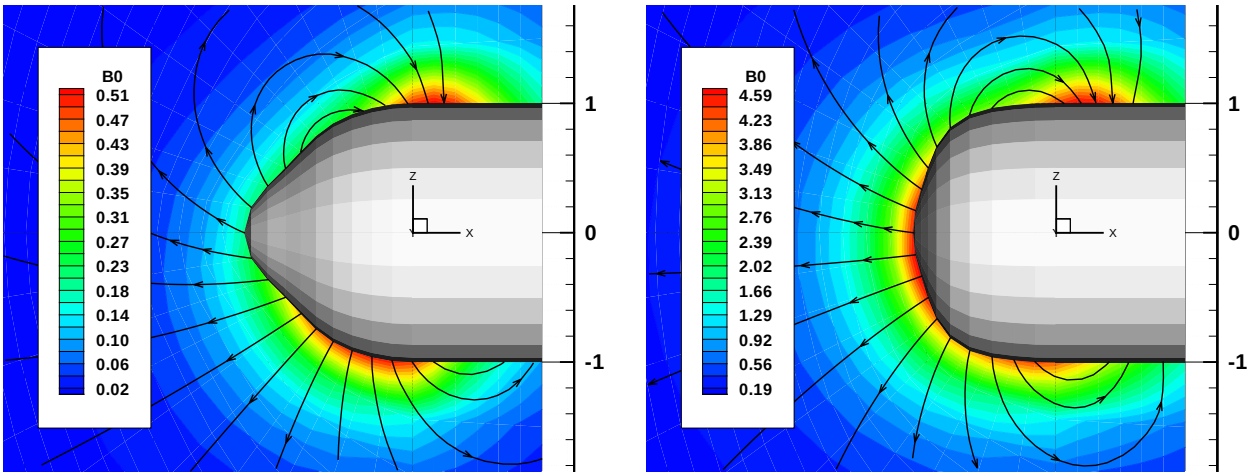

(a) C_D minimization

(b) C_D maximization

Figure 6. Optimal solutions.

VII. Conclusions

In this paper we have extended the discrete adjoint theory to the control of an inviscid hypersonic flow in the presence of strong magnetic fields using the ideal MHD governing equations.

Further work needs to be done in order to incorporate non-ideal MHD effects, such as the viscous Navier-Stokes terms and the magnetic dispersive terms in the equations.

In addition, there is still room for improvement of the flow solver efficiency, in particular, by substituting the explicit integration scheme by an implicit method since the former performs poorly when large magnetic fields produce extremely fast magneto-acoustic waves. In this case, the explicit time step becomes extremely small due to the CFL condition, limiting the usefulness of the numerical model. By doing so, the disadvantage of the finite-difference approach over the discrete adjoint would not be so large, but still orders of magnitude worse, but the overall design framework 1 efficiency would improve significantly.

The authors also plan to parallelize both the current flow and adjoint solvers to allow for larger, and thus, more realistic design problems.

Lastly, taking advantage of using a discrete adjoint approach, a move from the tedious and error prone differentiation of the adjoint system of equations (14) by hand to an automatic differentiation (AD) tool is planned. This is already been proved feasible for the Euler equations[23] and there are a few software packages available[24, 25] that will be tested for this purpose.

VIII. Acknowledgments

The authors are grateful for Air Force Office of Scientific Research contract No. AF04-009-0078 under tasks monitored by John Schmisseur. The first author also acknowledges the support of the *Fundação para a Ciência e a Tecnologia* from Portugal.

References

[1]Hallion, R. P., "The History of Hypersonics: or, Back to the Future – Again and Again," *AIAA Paper* 2005-0329, Jan. 2005, Proceedings of the 43^{rd} AIAA Aerospace Sciences Meeting and Exhibit, Reno, NV.

[2]Gurijanov, E. P. and Harsha, P. T., "AJAX: New Directions in Hypersonic Technology," *AIAA Paper* 1996-4609, Nov. 1996, Proceedings of the 7^{th} AIAA International Space Plane and Hypersonic Conference, Norfolk, VA.

[3]NASA, "X-43A Hypersonic Scramjet-Powered Research Aircraft," www.nasa.gov/missions/research/x43-main.html.

[4]Augustinus, J., Hoffmann, K. A., and Harada, S., "Numerical Solutions of Ideal MHD Equations for a Symmetric Blunt Body at Hypersonic Speeds," *AIAA Paper* 1998-0850, Jan. 1998, Proceedings of the 36^{th} AIAA Aerospace Sciences Meeting and Exhibit, Reno, NV.

[5]Poggie, J. and Gaitonde, D. V., "Computational Studies of Magnetic Control in Hypersonic Flow," *AIAA Paper* 2001-0196, Jan. 2001, Proceedings of the 39^{th} AIAA Aerospace Sciences Meeting and Exhibit, Reno, NV.

[6]Walters, R. W., Cinnella, P., Slack, D. C., and Halt, D., "Characteristic-based Algorithms for Flows in Thermo-Chemical Nonequilibrium," *AIAA Paper* 1990-0393, Jan. 1990, Proceedings of the 28^{th} AIAA Aerospace Sciences Meeting, Reno, NV.

[7]Shang, J. S., Gaitonde, D. V., and Updike, G. A., "Modeling Magneto-Aerodynamic Actuator for Hypersonic Flow Control," *AIAA Paper* 2004-2657, June 2004, Proceedings of the 35^{th} AIAA Plasmadynamics and Lasers Conference, Portland, OR.

[8]Gaitonde, D. V., "Simulation of Local and Global High-Speed Flow Control with Magnetic Fields," *AIAA Paper* 2005-0560, Jan. 2005, Proceedings of the 43^{rd} AIAA Aerospace Sciences Meeting and Exhibit, Reno, NV.

[9]Marta, A. C., Alonso, J. J., and Tang, L., "Automatic Magnetohydrodynamic Control of Hypersonic Flow Using a Discrete Adjoint Formulation," *AIAA Paper* 2006-0370, Jan. 2006, Proceedings of the 44^{th} AIAA Aerospace Sciences Meeting & Exhibit, Reno, NV.

[10]Powell, K. G., Roe, P. L., Myong, R. S., Gombosi, T., and Zeeuw, D. D., "An upwind scheme for magnetohydrodynamics," *12^{th} AIAA Computational Fluid Dynamics Conference, San Diego, CA, June 19-22, 1995*, Collection of Technical Papers. Pt. 1 (A95-36501 09-34), American Institute of Aeronautics and Astronautics, Washington, DC, 1995, pp. 661–674, AIAA Paper 1995-1704.

[11]Ramshaw, J. D., "A Method for Enforcing the Solenoidal Condition on Magnetic Field in Numerical Calculations," *Journal of Computational Physics*, Vol. 52, No. 3, Dec. 1983, pp. 592–596.

[12]Brackbill, J. U. and Barnes, D. C., "The Effect of Nonzero $\nabla \cdot B$ on the Numerical Solution of the Magnetohydrodynamic Equations," *Journal of Computational Physics*, Vol. 35, No. 3, May 1980, pp. 426–430.

[13]Panofsky, W. K. and Phillips, M., *Classical Electricity and Magnetism*, Addison-Wesley, 1962.

[14]Vinokur, M., "A Rigorous Derivation of the MHD Equations Based Only on Faraday's and Ampères's Laws," Nasa Ames Research Center, presentation at the LANL MHD Workshop, 1996.

[15]Tóth, G. and Odstrčil, D., "Comparison of Some Flux Corrected Transport and Total Variation Diminishing Numerical Schemes for Hydrodynamic and Magnetohydrodynamic Problems," *Journal of Computational Physics*, Vol. 128, No. 1, Oct. 1996, pp. 82–100.

[16]Tanaka, T., "Finite Volume TVD Scheme on an Unstructured Grid System for Three-Dimensional MHD Simulation of Inhomogeneous Systems Including Strong Background Potential Fields," *Journal of Computational Physics*, Vol. 111, No. 2, April 1994, pp. 381–389.

[17]Reuther, J. J., Jameson, A., Alonso, J. J., Rimlinger, M. J., and Saunders, D., "Constrained Multipoint Aerodynamic Shape Optimization Using an Adjoint Formulation and Parallel Computers, Part 1," *Journal of Aircraft*, Vol. 36, No. 1, 1999, pp. 51–60.

[18]Martins, J. R. R. A., Alonso, J. J., and Reuther, J. J., "Complete Configuration Aero-Structural Optimization Using a Coupled Sensitivity Analysis Method," *AIAA Paper* 2002-5402, Sept. 2002, Proceedings of the 9th AIAA/ISSMO Symposium on Multidisciplinary Analysis and Optimization, Atlanta, GA.

[19]Powell, K. G., Roe, P. L., Linde, T. J., Gombosi, T. I., and Zeeuw, D. L. D., "A Solution-Adaptive Upwind Scheme for Ideal Magnetohydrodynamics," *Journal of Computational Physics*, Vol. 154, No. 2, Sept. 1999, pp. 284–309.

[20]Balay, S., Buschelman, K., Gropp, W. D., Kaushik, D., Knepley, M. G., McInnes, L. C., Smith, B. F., and Zhang, H., "PETSc Web page," 2001, http://www.mcs.anl.gov/petsc.

[21]Gill, P. E., Murray, W., and Saunders, M. A., "SNOPT: An SQP Algorithm for Large-Scale Constrained Optimization," *SIAM Journal on Optimization*, Vol. 12, No. 4, Dec. 2002, pp. 979–1006.

[22]Hicks, R. M. and Henne, P. A., "Wing Design by Numerical Optimization," *AIAA Journal*, Vol. 15, No. 7, July 1978, pp. 407–412.

[23]Martins, J., Alonso, J., and van der Weide, E., "An Automated Approach for Developing Discrete Adjoint Solvers," *AIAA Paper* 2006-1608, May 2006, Proceedings of the 47^{th} AIAA/ASME/ASCE/AHS/ASC Structures, Structural Dynamics, and Materials Conference, Newport, RI.

[24]Dervieux, A., Hascoet, L., Pascual, V., Koobus, B., and Vazquez, M., "TAPENADE Web page," 2005, http://www-sop.inria.fr/tropics/tapenade.html.

[25]Bischof, C., Carle, A., Hovland, P., Khademi, P., and Mauer, A., "ADIFOR 2.0 User's Guide (Revision D)," Tech. Rep. Technical Memorandum No.192, Argonne National Laboratory, 1998.